Endocranial Casts of Camelops hesternus and Palaeolama sp.: New Insights into the Recent History of the Camelid Brain

Ana Balcarcel, Dylan Bastiaans, Maeva J Orliac

Brain, Behavior and Evolution

Original Paper

Brain Behav Evol 2023;98:107–120
DOI: 10.1159/000528762

Received: February 20, 2022
Accepted: December 12, 2022
Published online: December 27, 2022

Endocranial Casts of *Camelops hesternus* and *Palaeolama* sp.: New Insights into the Recent History of the Camelid Brain

Ana M. Balcarcel[a] Dylan Bastiaans[a] Maeva J. Orliac[b]

[a]Palaeontological Institute and Museum, University of Zurich, Zurich, Switzerland; [b]Institut Des Sciences de L'Évolution de Montpellier, Université de Montpellier, CNRS, EPHE, IRD, Montpellier, France

Keywords
Artiodactyl · Mammal · Cerebral cortex · Pleistocene · Fossil · Endocast

Abstract
Endocranial casts are capable of capturing the general brain form in extinct mammals due to the high fidelity of the endocranial cavity and the brain in this clade. Camelids, the clade including extant camels, llamas, and alpacas, today display high levels of gyrification and brain complexity. The evolutionary history of the camelid brain has been described as involving unique neocortical growth dynamics which may have led to its current state. However, these inferences are based on their fossil endocast record from approximately ~40 Mya (Eocene) to ~11 Mya (Miocene), with a gap in this record for the last ~10 million years. Here, we present the first descriptions of two camelid endocrania that document the recent history of the camelid brain: a new specimen of *Palaeolama* sp. from ~1.2 Mya, and the plaster endocast of *Camelops hesternus*, a giant camelid from ~44 to 11 Kya which possessed the largest brain (~990 g) of all known camelids. We find that neocortical complexity evolved significantly between the Miocene and Pleistocene Epochs. Already ~1.2 Mya the camelid brain presented morphologies previously known only in extant taxa, especially in the frontal and parietal regions, which may also be phylogenetic informative. The new fossil data indicate that during the Pleistocene, camelid brain dynamics experienced neocortical invagination into the sagittal sinus rather than evagination out of it, as observed in Eocene to Miocene taxa.

Introduction

The evolutionary history of the mammalian brain is known from studies of the fossil record of endocranial casts [Edinger, 1966; Dechaseaux, 1969; Jerison, 1971; Macrini, 2009; Rowe et al., 2011; Orliac and Gilissen, 2012] which can capture brain size, shape, and often the neocortical topology [Dechaseaux, 1962; Edinger, 1966; Dechaseaux, 1968; Repérant, 1971b; Jerison, 1977; Dozo, 1998; Rowe et al., 2005; Jerison, 2007; Macrini, 2009; Rowe et al., 2011; Orliac and Gilissen, 2012] due to the high fidelity of the endocranial cavity and the brain mammalian brain. Endocasts can be natural, created by normal

Karger@karger.com
www.karger.com/bbe

Correspondence to:
Ana M. Balcarcel, ana.balcarcel@gmail.com

fossilization processes, or man-made, by casting fossil endocrania, physically or virtually. Brain complexity has reached exceptional levels in humans and other primates but is closely followed by members of Artiodactyla [Lewitus et al., 2014], the clade including cetaceans (whales, dolphins, and porpoises) and artiodactyls (i.e., ruminants, pigs, camels) [Hassanin et al., 2012]. Among the latter, camelids, which include extant camels, guanacos, and vicuñas, were one of the first lineages to increase their neocortical complexity in the Eocene (~40 Mya) [Orliac and Gilissen, 2012]. Today, the camelid brain displays remarkable differentiation of the sulcal system and significant expansion of the neocortex, particularly of the peripheral brain (gyrus 2), compared to other mammals [Repérant, 1971b, a].

The physical dynamics by which camelids may have evolved their current brain form is reportedly unique among mammals [Repérant, 1971a]. In most mammals, the neocortex reportedly develops from the midline outward towards the lateral brain. In contrast, the camelid neocortex reportedly develops by invagination of the telencephalon into the sagittal sinus [Repérant, 1971a]. Evidence for developmental invagination is provided by prenatal ontogenetic studies showing "primitive" sulci in the sagittal plane; and evolutionary invagination has been hypothesized based on the camelid fossil endocast record, and the reported sequence of sulcal development throughout geological time [Repérant, 1971a, b]. Brain form and neocortical topologies have been described for camelids from the Eocene, Oligocene, and Miocene Epochs (Fig. 1a–c), revealing the pattern of deep-time brain evolution in this group from approximately ~40 to ~11 million years ago. Since then, there has been a void in their fossil endocast record, limiting our understanding of the mode and tempo in which this lineage reached their current brain morphology.

Here, we present the first descriptions of Pleistocene camelid endocasts from two different stages. The first is a natural endocranial cast of a newly discovered *Palaeolama* sp. from the mid-Pleistocene (~1.2 Mya) of South America, and the second, a plaster endocast of the skull of *Camelops hesternus* from the late Pleistocene (~44 Kya to 11 Kya) of North America. *Palaeolama* is likely the closest fossil relative of extant South American camelids, *Lama* and *Vicugna*, according to the latest systematic review of Camelinae [Lynch et al., 2020], and our specimen represents the earliest occurrence of this genus in the fossil record [Scherer, 2012; Lynch et al., 2020]. The genus *Camelops* contains some of the largest camelids ever known, often referred to as the "giant camels" [Zazula et al., 2011], and is one of the most studied camelid taxa [Leidy, 1873; Hay, 1913; Webb, 1965; Jerison, 1971; Humpula et al., 2007; Heintzman et al., 2015; Baskin and Thomas, 2016; Lynch et al., 2020]. Its endocast has been referred to in one prior publication [Jerison, 1971] but has never been described. The phylogenetic position of genus *Camelops* remains much debated today, notably due to differences between molecular and morphology-based trees which place it either closer to South American taxa or to Asian camelids [Scott and Jepsen, 1940; Harrison, 1979; Honey et al., 1998; Heintzman et al., 2015; Baskin and Thomas, 2016] (Fig. 1d). Endocranial characters can be an important data source for phylogenetic inference [Macrini et al., 2007]. Here, we describe characters of potential phylogenetic importance to clarify the position of *Camelops* within Camelidae [Harrison, 1979; Honey et al., 1998; Scherer, 2012; Heintzman et al., 2015; Baskin and Thomas, 2016].

Materials and Methods

Materials

The endocast of *Palaeolama* sp., PIMUZ A/V 409, is a natural cranial endocast. It belongs to the Roth collection ("Katalog der Non-Xenarthra der Rothschen Sammlung") of the Palaeontological Institute and Museum of the University of Zurich (PIMUZ) and dates to the Pampeano Inferior (Ensenadan), approximately ~1.95/1.77 Mya to 0.4 Mya [Verzi et al., 2004; Lynch et al., 2020] from the "San Lorenzo 2" locality in Argentina [Roth, 1889; Schulthess, 1920]. The specimen includes multiple large skull fragments fitting anterior and posterior facets of the endocast, and various rostral and dental fragments that fit the rest of the skull. The endocast of *C. hesternus*, LACM 4700-1, is a plaster cranial endocast from a *C. hesternus* skull with catalogue number HC692, both belonging to the Rancho La Brea Tar Pits (RLBTP) in California, USA (A. Farrell, RLBTP, pers. comm.). The *C. hesternus* skull is dated between ~44 Kya and 11 Kya (Rancholabrean) [Rook et al., 2019]. No other data are available for this specimen, and it has not been described except as mentioned in a quantitative study by Jerison [1971] (A. Farrell, RLBTP, pers. comm.). Interactive three-dimensional images of the endocast were provided in Adobe Portable Document Format (Adobe® Acrobat® v. 2021.007.20091) by the Rancho La Brea Tar Pits collections staff.

The geological age of *Procamelus* is based on new data acquired during our investigations. This datum was relevant for the section on brain size evolution. Previous studies on camelid brain size [Jerison, 1971], neocortical anatomy [Repérant, 1971a], and rate of brain size evolution [Kruska, 1982] have referred to the same *Procamelus* specimen (AMNH F:AM 40366) used here as an early or late Pliocene specimen. This specimen was first illustrated and published by Edinger [1966] as an "early Pliocene *Procamelus*" [Edinger 1966, p. 157–158], but without a catalogue number. The same specimen was described as a Pliocene taxon by Repérant [1971] (J. Repérant, pers. comm.). Based on textual references, this is the same specimen that Jerison [1971] identified as AMNH F:AM 40366: "a new and hitherto undescribed

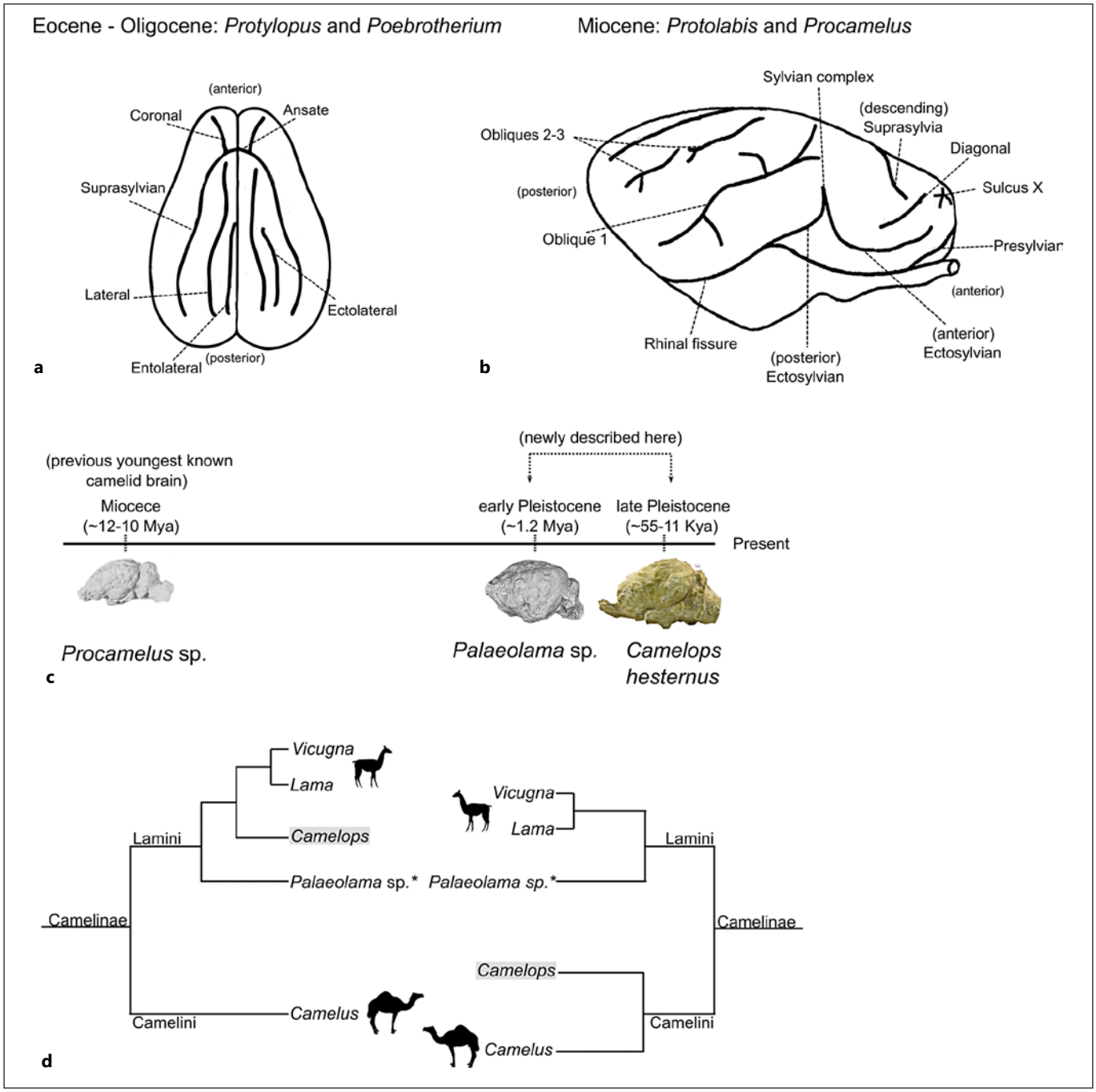

Fig. 1. a Schematic of the camelid brain from Eocene to Oligocene, and (**b**) Miocene. Adapted from Repérant [1971]. **c** Geological timeline for endocasts described here. *Procamelus* outline based on Edinger [1966], elements not to scale. **d** Phylogenetic hypotheses for *Camelops,* based on Scherer [2012]; Lynch et al. [2020]. * PIMUZ A/V 4091 is referred to *Palaeolama* sp. [Lynch et al., 2020].

specimen from the Frick Collection of the American Museum of Natural History" [Jerison 1971, p.228]. The American Museum of Natural History (AMNH) confirms that AMNH F:AM 40366 is a Miocene *Procamelus* from the Clarendonian North American Land Mammal age (NALMA), dated to ~12.5 Mya to 9.4 Mya [Barnosky et al., 2014] of the Valentine Formation Burge Member (C. Mehling, AMNH, pers. comm.), and we refer to it as such in this study (Fig. 1b).

Methods

The skull and dental elements of the specimen PIMUZ A/V 4091 are first briefly described in order to evaluate their referral to *Palaeolama* sp. in the PIMUZ collections catalogue. To improve visualization of the neocortex, the endocast was scanned via X-ray computed tomography (CT) at the University of Montpellier using an EasyTom 150 μ-CT scanner at 92 KV with a resulting resolution of 70 μm. Digital reconstruction of the scan and segmentation to remove remaining cranial bone was executed in Avizo (v. Lite 9.0.1) (Thermo Fisher Scientific-FEI). A small portion of the right parietal region could not be segmented successfully due to a lack of contrast between cranial bone and endocast. The 3D interactive images of the endocast of *C. hesternus,* LACM 4700-1, were examined in Adobe Acrobat Reader DC (Adobe®Acrobat® v. 2021.007.20091). Models (3D) are available for visualization and free download at MorphoMuseuM.com [Lebrun and Orliac, 2016].

The anatomical terminology used for neocortical descriptions is presented in Table 1 and includes our proposed equivalence of terms from prior studies including Dechaseaux [1962], Herre and Thiede [1965], Edinger [1966], Dechaseaux [1969], Repérant [1971], and Barone and Belemlih [1973]. Interpretations of sulcal homologies are based on macroscopic morphological observations and sulcal maps in previous publications on this subject [Dechaseaux, 1962, 1968, 1969; Repérant, 1971b, a; Barone and Belemlih, 1973; Dechaseaux, 1973]. Linear measurements of all specimens were taken in Meshlab (v.2021.05) or Affinity Photo (v.1.9.2.1035) following Macrini [2009] [Cignoni et al., 2020]. For comparisons of encephalization, body mass estimates for *Palaeolama* sp. and *C. hesternus* were calculated using four separate body mass prediction equations from Janis [1990] and Damuth and MacFadden [1990], based on upper molar dimensions [Damuth and MacFadden, 1990; Janis, 1990]. The arithmetic mean of these results was used to calculate encephalization quotients (EQs) as per Jerison [1970]. We equate grams and millilitres for comparison purposes. Brain and body size data for extant camelids and other EQ data were taken from Jerison [1971] as noted.

Results

Systematic Paleontology
Tylopoda Illiger, 1811.
Camelidae Gray, 1821.
Palaeolama Gervais, 1869.

Description: *Palaeolama* sp. Skull and Teeth

The specimen includes parts of the anterior and posterior cranium which articulate with the endocast but not to each other. The anterior section contains portions of the frontals, orbits, and proximal rostrum (Fig. 2a–c). In dorsal view, the skull's overall shape is similar to that of extant SACs, narrowing sharply from the orbits towards the anterior rostrum. Left and right upper molars (M2-M3), which were reconstructed from multiple fragments by the first author, are high-crowned and selenodont (Fig. 2d). In the maxilla, transverse sections of the roots of P4-M1 are exposed and there is no indication of a P3 alveolus. A diastema extends mesially from position P4. Isolated fragments of the anterior rostrum contain parts of two caniniform, recurved teeth separated by a diastema of approximately ~3.5 cm, suggesting these are likely the third upper incisor (I3) and upper canine (C) (Fig. 2e–f) [Lynch et al., 2020]. The catalogue identification of *Palaeolama* sp. is supported by the presence of several characters diagnostic of South American Lamini (Camelidae) including the shape and extent of the choanae, which reach beyond the distal edge of M2 (Fig. 2a) [Scherer, 2012; Lynch et al., 2020]. Its geographic and stratigraphic provenance also supports membership in Lamini. The presence of an I3, a recurved and laterally compressed upper canine, and a shallow maxillary fossa (Fig. 2b) define it further as within or close to *Palaeolama* [Harrison, 1979]. We refer to this specimen as *Palaeolama* sp. in the entirety of this study, based on its catalogue data and these observations, while recognizing that a phylogenetic analysis is lacking [Webb, 1965; Scherer, 2012; Lynch et al., 2020].

Description: Endocast of *Palaeolama* sp., PIMUZ A/V 4091

General morphology: The natural endocast of PIMUZ A/V 4091 is nearly complete and minimally distorted (Fig. 3a, c), missing olfactory bulbs and most of the ventral surface. In dorsal view, it has an ovoid outline, narrower anteriorly than caudally, as is typical of camelid brains [Herre and Thiede, 1965; Repérant, 1971a]. Bifurcation of the frontal lobes forms a wide v-shaped gap. The posterior two-thirds of the cerebral portion of the endocast is nearly uniform in width (Fig. 3b). In lateral view (Fig. 3d), the dorsal outline slopes downward from its apex in the caudal cerebrum to the prefrontal margin of the endocast. A nearly complete cerebellar cast comprises approximately one-quarter to one-third of the total endocast length (excluding missing olfactory bulbs). Measurements of general endocast dimensions are in Table 2.

Telencephalon: The cast of the neocortex of *Palaeolama* sp. presents a greater number of sulci than earlier known fossil camelids, and comparatively, an expansion of both lateral and prefrontal neocortical regions. The coronal and suprasylvian sulci (anterior, middle, and posterior portions), considered to be "archaic" [Repérant, 1971a], are visible on the dorsal surface of the endocast (Fig. 3b). The suprasylvian sulcus is observed best on the left cerebral hemisphere. It is long and mostly longitudinal, curving around and beyond the coronal sulcus at the anterior endocast, and bifurcating into anterior and descending

Table 1. Anatomical terminology used in current study and equivalent terms in prior studies

Current study	Reperant [1971 a,b]	Barone and Belemlih [1973]	Edinger [1966]	Herre and Thiede [1965]	Dechaseaux [1962, 1969]
Coronal	Coronal	Coronalis and postcoronalis	–	Sulcus coronalis	Coronal
Transverse Coronal	Branche tranverse du Coronal (c1t)	–	–	–	–
Lateral	Latérale	Marginalis	–	Sulcus lateralis	Latéral
Anterior Suprasylvian middle Suprasylvian posterior Suprasylvian	Suprasylvien (antérieure, moyenne, postérieur)	Suprasylvius rostralis/ medius/caudalis	–	Sulcus suprasylvius	Suprasylvia
Descending Suprasylvian	(branche descendente) Suprasylvien	Suprasylvius rostralis	–	–	–
Ansate	Ansate	Ansatus	Transverse sulcus	Sulcus transversus	Crucial
Entolateral	Entolatéral	–	–	Sulcus entolateralis	–
Ectolateral and accessory ectolaterals	Ectlolatéral principal + ectolatérales accessoires	Ectomarginalis	–	Sulcus ectolateralis	–
Sulcus X	Sillon X	–	–	–	Sillon "upsilon"
Rhinal fissure (anterior and posterior branches)	Scissure rhinale: rameaux aboral, postérieure de "rhinale postérieure" (rh.p.p, rh.p.s); "rhinale antérieure" (rh.a), rameau oral de rhinale antérieure (rh.p.a)	Sulcus rhinalis lateralis pars rostralis + Sulcus rhinalis lateralis pars caudalis	Fissura palaeo-neocorticalis or fissura rhinica	Sulcus rhinalis and Sulcus proreus	Rhinale antérieure + postérieure
Sagittal sinus*	Sinus sagittalis	–	–	–	–
Sylvian complex	Complex sylvien	Fissura lateralis cerebri	–	Lateralis cerebri, acuminis	Complexe sylvien
Presylvian	Presylvia	–	–	Praesylvius	Presylvia
Anterior Ectosylvian	Ectosylvia antérieure (e.a.h)	Subsylvius	–	Lateralis cerebri, anterior	Ectosylvia antérieure
Posterior Ectosylvian	Ectosylvia postérieure (e.p.)	–	–	Lateralis cerebri, posterior	Ectosylvia postérieure
Ascending anterior Ectosylvian	Ectosylvia antérieure, rameau ascendente (r.a.e.a)	–	–	–	–
Obliques 1, 2, 3	Obliques 1, 2, 3	Suprasylvius caudalis + Ectosylvius caudalis	–	Ectosylvius	–
Diagonal	Diagonal	Suprasylvius rostralis	–	–	–
Arched sulcus	Sillon arqué	Ectosylvius rostralis	–	Anterior Ectosylvius	Sillon "delta"
Accessory Sylvian complex	Complex sylvien accessoire	–	–	–	–
Intercalaire	Intercalaire/splenial	Cruciatus	–	–	–

* Also known as superior sagittal sinus (Macrini et al., 2007).

Brain Behav Evol 2023;98:107–120
DOI: 10.1159/000528762

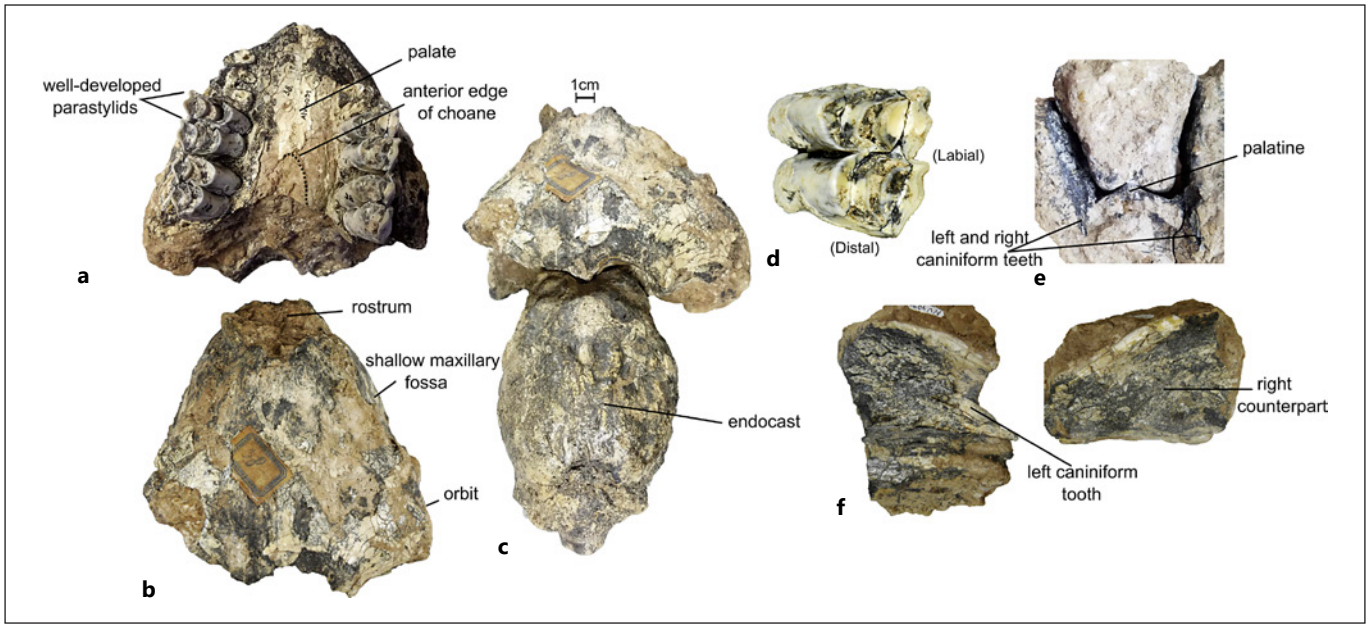

Fig. 2. PIMUZ A/V 4091, all elements: (**a**) palate and teeth; (**b**) anterior skull fragment, dorsal view; (**c**) articulated skull and endocranial cast, dorsal view; (**d**) left M2; (**e**) anterior snout in transverse section; (**f**) anterior snout fragments, disarticulated, medial views. Scale bar for part "c" only.

branches (Fig. 3b). The coronal is a single longitudinal sulcus, with the transverse ansate crossing it perpendicularly. Medial to the suprasylvian sulcus is the ectolateral sulcus [Herre and Thiede, 1965; Repérant, 1971a], also preserved best on the left hemisphere. Between the ectolateral sulcus and the sagittal sinus (Fig. 3b), several short furrows in no particular orientation appear to be fragments of accessory ectolateral sulci. At the anterior-most edge of the prefrontal, *Palaeolama* sp. presents an intercalaire sulcus (Fig. 3b, e), a short curvilinear furrow just anterior to the proximal end of the suprasylvian sulcus.

In lateral view, the neopallium possesses a well-marked ectosylvian sulcus, with curvilinear anterior and posterior branches that join at the sylvian complex (Fig. 3b). Oblique sulci 1–3 are positioned caudally in the posterior third of the lateral surface of the endocast (Fig. 3d). Oblique sulcus 1 is the longest and most continuous, and oblique sulcus 3 appears mostly rectilinear. The anterior rhinal fissure is not preserved, nor is the region immediately dorsal to it where we would expect to find the presylvia and diagonal sulci [Repérant, 1971b]. In oblique view, sulcus X – shaped just like its name – is just lateral to the intercalaire sulcus (Fig. 3e). Below the suprasylvian sulcus and above the sylvian complex, we observe the arched sulcus – an arrangement of at least three curvilinear boughs [Repérant, 1971a] (Fig. 3e). On the ventral side of the endocast, the pyriform lobes appear small and slightly convex.

Mesencephalon: The tectum of the mesencephalon is not dorsally exposed, fully covered by the posterior expansion of the neocortex (telencephalon) (Fig. 3a).

Metencephalon: Dorsally, the metencephalon is the narrowest region of the endocast (Fig. 3a, b). The cerebellum is nearly half as wide as the cerebrum and particularly short in comparison to the latter. The cerebellar hemispheres are obscured by a salient superior petrosal sinus and their shape and extension cannot be determined precisely (Fig. 3d). However, the cast of the cerebellum indicates that the vermis was much wider than the hemispheres. Parafloccular lobes project laterally, and the internal acoustic meatus is visible (Fig. 3c–d).

Encephalization Quotient: Here, based on dental measurements (see SD1), we estimate that *Palaeolama* sp. had a body mass of ~264.5 kg yielding an EQ of 0.90 following Jerison's equation [Jerison, 1970] (SD1).

Systematic Paleontology
Tylopoda Illiger, 1811
Camelidae Gray, 1821
Camelops Leidy, 1854
Camelops Hesternus Leidy [1873].

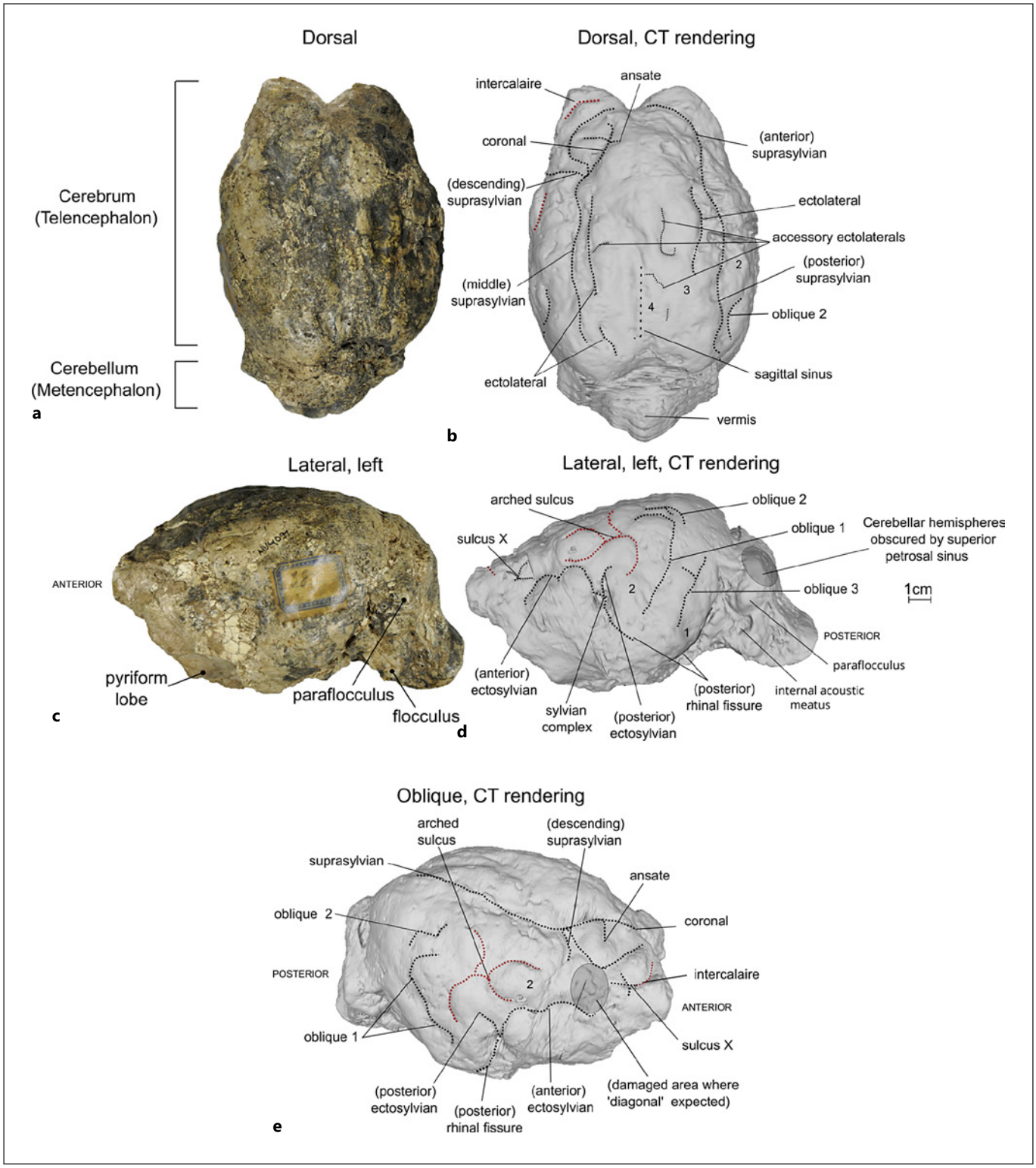

Fig. 3. Endocranial cast of *Palaeolama* sp., PIMUZ A/V 4091: (**a**) dorsal view, natural endocast, (**b**) dorsal view, digital endocast, (**c**) lateral left, natural endocast, (**d**) lateral left, digital endocast, (**e**) anterior oblique (reflected image), digital endocast. Dotted lines = sulci. Sulci new to Pleistocene camelids in red. Numbers 1–4: gyri. Scale bar specific to part "d". CT, computed tomography.

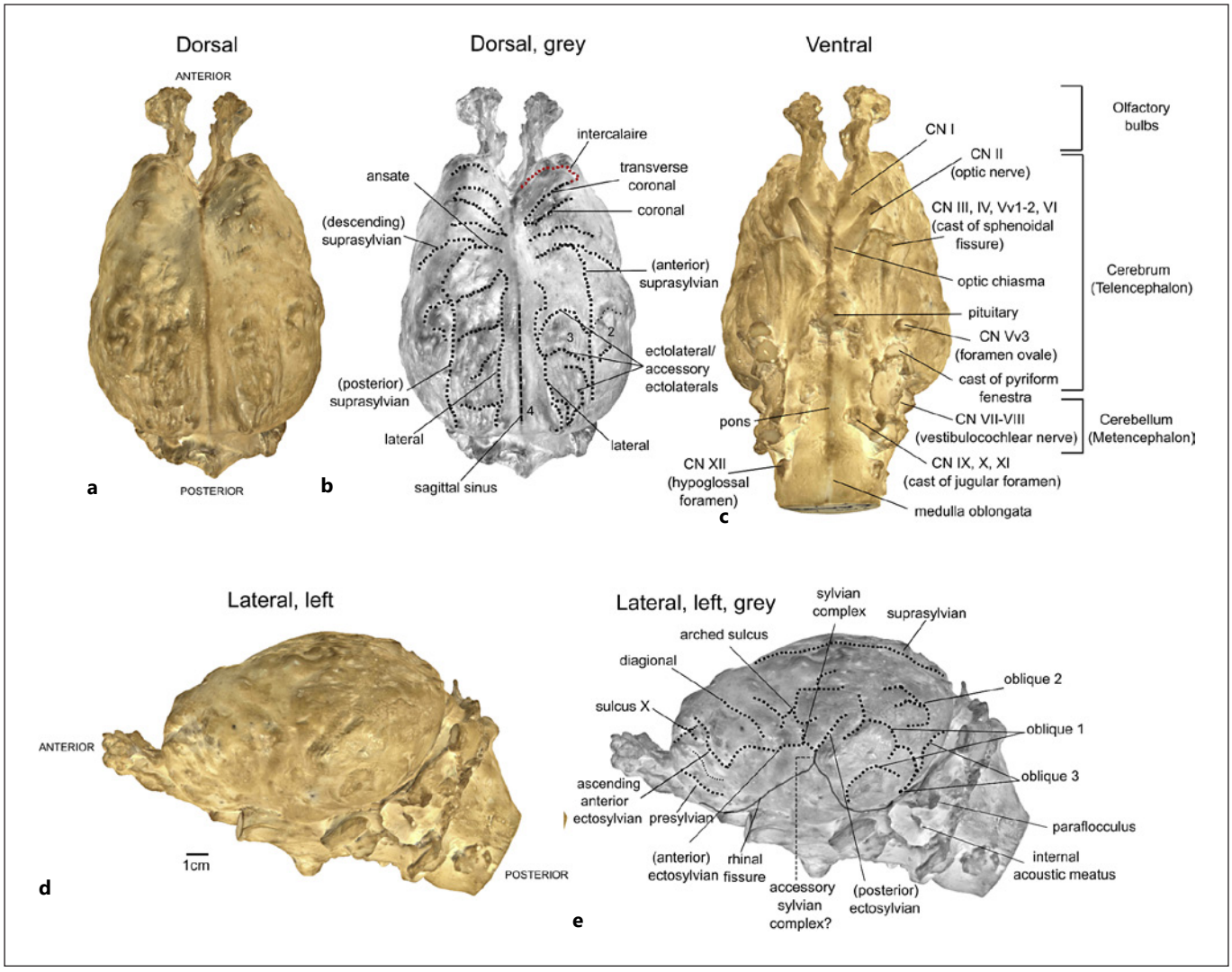

Fig. 4. Endocranial cast of *Camelops hesternus*, LACM-4700-1: (**a**) dorsal view, (**b**) dorsal view with sulci identified, (**c**) ventral view, (**d**) lateral view, left, (**e**) lateral view, left, with sulci identified. Dotted lines = sulci. Solid line = rhinal sulcus. Sulci new to Pleistocene in red. Numbers 1–4: gyri. CN, cranial nerve.

Table 2. Cranial endocast dimensions and brain/body mass estimates for *Camelops* and *Palaeolama* sp. described herein

Taxon	Specimen	Age	TEL, mm	CL, mm	CW, mm	CH, mm	OBL, mm	CBL, mm	CBW, mm	CBH, mm	Estimated endocast volume, g	Estimated body mass, kg**
C. hesternus	*LACM 4700-1*	55-11 Kya	192.1	116	111.3	114.8	51.5	4.33	72.45	85.5	990*	825.9
Palaeolama sp.	*PIMUZ A/V 4091*	1.2 Mya	137.8	93.6	85.4	77.7	na	37.2	64	49	444.3	263.5

Measurements follow Macrini (2009). TEL, total endocast length; CL, cerebral length (without olfactory bulbs); CW, cerebral width; CH, cerebral height; OBL, olfactory bulb length; OBW, olfactory bulb width; CBL, cerebellar length; CBW, cerebellar width; CBH, cerebellar height. * From Jerison [1971]. ** Calculations in online supplementary file SD1, available at www.karger.com/doi/10.1159/000528762.

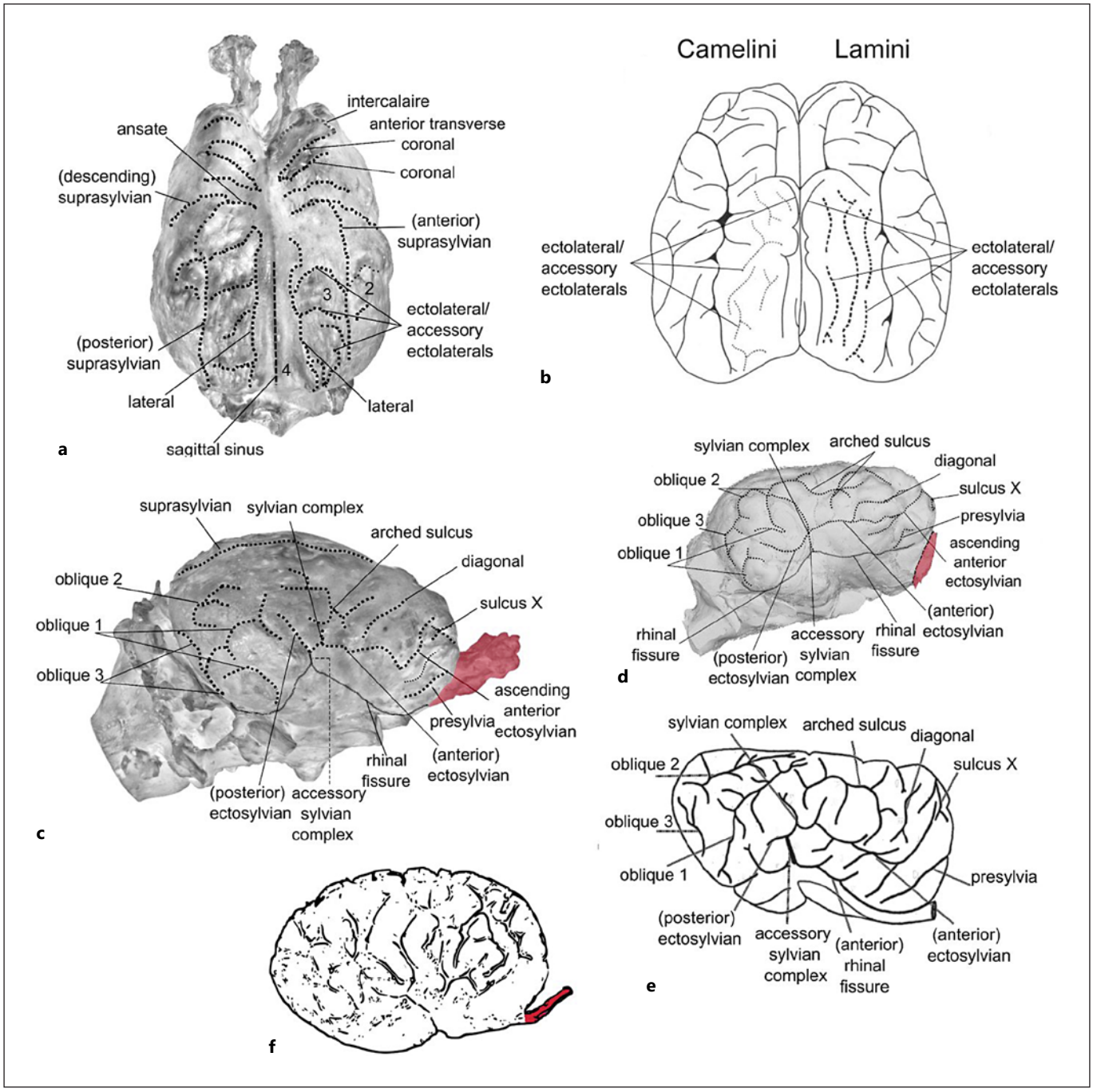

Fig. 5. Comparison of *Camelops hesternus* versus extant camelid cranial endocasts. **a**, **b** *C. hesternus* in (**a**) dorsal and (**b**) lateral views; (**c**) specific features of Camelini and Lamini based on Repérant (1971b: Fig. 3), dorsal view; (**d**) *Vicugna vicugna*, lateral view; (**e**) *Camelus* sp. based on Repérant (1971b: Fig. 3), lateral view; (**f**) *Camelus* sp. based on Barone and Belemlih (1973: Fig. 6), lateral view. Dotted lines = sulci. Solid lines = rhinal sulcus. Dashed line = circular fissure.

Description: Endocast of C. Hesternus, LACM-4700-1

General morphology: The natural endocast of *C. hesternus* is complete, includes olfactory bulbs, and appears undistorted. The cerebral cast is pear-shaped in dorsal view, narrower at its anterior, but somewhat more rectangular than *Palaeolama* sp. in all views (Fig. 4a–e). Anterior

frontal lobes are bifurcated by a wide gap. Cerebellar cast length is approximately one-fifth of the cerebral cast length. Measurements of general endocast dimensions are in Table 2.

Telencephalon: In dorsal view (Fig. 4a–b), the olfactory bulbs are elongated, pedunculated, and ovoid-shaped. The ethmoidal chamber, also known as the ethmoidal fossa [Rowe et al., 2005], is rather narrow and pierced by the dense sieve of the cribriform plate, visible in ventral view (Fig. 4c). Between the anterior and posterior parts of the neocortex, the rectilinear anterior and descending branches of the suprasylvian sulcus split and simultaneously converge with the short transverse ansate, which turns medially into the sagittal sinus at this point. The coronal sulcus here has at least one additional branch: the anterior transverse coronal sulcus and the intercalaire sulcus are present just anterior to them. A rectilinear fold closest to the midline and parallel to the sagittal sinus – which was not observable in the *Palaeolama* endocast – is the lateral sulcus, considered an archaic feature of the camelid brain [Repérant, 1971a]. Between the lateral and the suprasylvian sulci, the ectolateral sulcus comprises a dense arrangement of short sulci mostly oriented transversely (Fig. 4b).

On the lateral surface of the endocast, *C. hesternus* has an ectosylvian sulcus with an additional branch stemming from its anterior end and rising towards the prefrontal cortex: the ascending anterior ectosylvian sulcus (Fig. 4d–e). The oblique sulci are curvilinear and converge into each other; while the arched sulcus is positioned more anteriorly than in *Palaeolama* sp. The rhinal fissure at the base of the cerebrum is fully preserved, with anterior and posterior branches joining at an acute angle at what appears to be the accessory sylvian complex – a short vertical furrow connecting the posterior ectosylvian sulcus to the posterior rhinal fissure – rather than at the sylvian complex [Repérant, 1971a] [see Repérant 1971, p. 663] (Fig. 4e). The presylvian sulcus is the obliquely oriented sulcus located just dorsal to the anterior rhinal fissure. In the prefrontal region, sulcus X is located just below the ascending anterior ectosylvian sulcus; and the diagonal sulcus is observable posterior to it.

Diencephalon: A cast of the pituitary is captured in ventral view (Fig. 4c–e). It is globular and strongly protrudes ventrally. Its posterior border is located at the level of the foramen ovale, and its anterior margin is at the level of the base of the optic chiasma.

Mesencephalon: The tectum of the mesencephalon is not dorsally exposed, fully covered by the posterior expansion of the neopallium.

Metencephalon: Dorsally, the metencephalon is the narrowest region of the endocast. As in *Palaeolama* sp., the cerebellum is nearly half as wide as the cerebrum and particularly short in comparison to the latter. The dorsal surface of the cerebellum is covered by wide sinuses which, together with the parietal/occipital suture, mask its external features. The imprints of the petrosal bones and the surrounding sinuses hide the cerebellar hemispheres. Only the width of the vermis can be appreciated and it represents half of the total width of the cerebellum. The pons-medulla oblongata continuum is long and widens posterior to the cast of the petrosal bones (Fig. 4c). The brainstem is particularly wide. Parafloccular lobes project laterally, and the internal acoustic meatus is visible (Fig. 4e).

Cranial nerve exits: The pattern of cranial nerve exits is completely accessible on LACM-4700-1 and strongly resembles that of *Lama* and *Camelus* provided by Repérant [1971a]. The optic chiasma lies shortly anterior to the cast of the sphenorbital fissure where the cranial nerves (CNs) III, IV, Vv1-2, and VI exit. The foramen ovale (exit of the mandibular division of the trigeminal nerve, CN Vv3) is rather small and opens at the level of the posterior margin of the pituitary. The pyriform fenestra is twice as wide as the foramen ovale and lies just posterior to it. It is connected to the jugular foramen (exit for CNs IX, X, XI) by a continuous basicochlear fissure. The hypoglossal foramen (exit for CN XII) is a small opening located on the lateral aspect of the brainstem, separated from the jugular foramen by a deep depression.

Encephalization quotient: Here, based on dental measurements (see online suppl. material, available at www.karger.com/doi/10.1159/000528762), we estimate that *C. hesternus*, had a body mass of ~825.9 kg, yielding an EQ of 0.94 according to Jerison's equation [Jerison, 1970] (SD1).

Discussion

Camelops Affinities

The phylogenetic position of genus *Camelops* is currently debated as being either within the clade Lamini (closer to *Lama*) or Camelini (closer to *Camelus*) (Fig. 1c). Morphological phylogenetic analyses predominantly place *Camelops* within the former [Harrison, 1979; Honey et al., 1998; Lynch et al., 2020], while genomic and proteomic analyses place it within the latter [Baskin and Thomas, 2016; Buckley et al., 2019]. The endocranial cast of *C. hesternus* shows morphological similarities with the

brain of extant *Camelus* (Camelini) and some with *Vicugna* (Lamini), to the exclusion of *Lama* (Lamini). Affinities with *Camelus* include the shape and extent of the olfactory bulbs and their relative proportion to the cerebrum. Like *Camelus*, *Camelops* shows rather elongated olfactory bulbs that do not about the anterior part of the cerebrum; whereas in *Lama* and *Vicugna*, the olfactory bulbs are stocky and closely opposed to the cerebrum (Fig. 5a–f). In ectolateral morphology, which is a significant feature of the dorsal neocortex for distinguishing Camelini and Lamini [Reperant 1971], *C. hesternus* is also more similar to *Camelus.* It has more transverse and oblique orientation of the ectolaterals compared to *Lama* and *Vicugna* where the ectolaterals are more longitudinal (Fig. 5a–e). The dorsoventral dimension of the prefrontal is similar between *C. hesternus* and both *Camelus* and *Vicugna*. The latter trait may be correlated with more forward-facing orbits and the evolution of binocular vision in other mammals [Barone and Belemlih, 1973]. Lastly, the superlative absolute size of the *Camelops* endocast (990 g) would also suggest a closer relationship to the larger brained *Camelus* (mean brain mass: 570–760 g) than to the South American genera (mean brain mass: 192–276 g) [Jerison, 1971] (SD1 and Table 2). These traits may be phylogenetically informative given a better assessment of intraspecific variation.

Camelid Brain Evolution: Documented History from Eocene to Present

The two new camelid endocasts described in this work document the most recent part of the history of brain evolution in Camelidae. The earliest known camelid, *Protylopus* [Wortman, 1898] of the Eocene (~40 Mya), had a small and simple neocortex restricted to the dorsal half of its endocast [Edinger, 1966], and is considered to represent the primitive camelid brain condition [Orliac and Gilissen, 2012] (Fig. 1a). It had an ovoid general shape and four main longitudinal sulci that are considered in the literature as "archaic" sulci [Repérant, 1971a]: the coronal, suprasylvian (single branch), lateral, and entolateral sulci. Throughout the Cenozoic, the camelid brain progressively enlarged, absolutely and relatively [Jerison, 1971], and increased neocortical folding of the lateral brain as seen by the early Oligocene in *Poebrotherium wilsoni,* which possessed anterior and posterior ectosylvian sulci, a sylvian complex, a descending suprasylvian sulcus, presylvian sulcus and oblique sulcus 1 [Repérant, 1971a]. By the late Oligocene, the dorsal brain had further evolved with the addition of an ectolateral sulcus as seen in *Poebrotherium labiatum* [Scott and Jepsen, 1940] (Fig. 1a). During the Miocene, *Protolabis* and *Procamelus* developed oblique sulci 2–3 in the posterior brain, while the diagonal sulcus and sulcus X marked evolution of the fronto-lateral region [Repérant, 1971a] (Fig. 1b).

Approximately one million years ago, *Palaeolama* sp. (~1.2 Mya) presented the first observed occurrence among camelids of the intercalaire and arched sulci (Fig. 3). These features were previously observed only in extant camelids and reflect an expansion of the surface area of prefrontal and parietal neocortices, respectively. The suprasylvian sulcus – primitive but variable among camelids [Repérant, 1971b, a] – is more convoluted, with anterior and lateral bifurcations in the anterior portion of the endocast. Also novel at this time is the multi-branched ectolateral sulcus of the dorsal neocortex, contrasting with the single, rectilinear ectolateral sulcus observed in *Procamelus* (Miocene), and earlier forms [Repérant, 1971a].

By the latter stages of the Pleistocene (~44 Kya – 11 Kya), *C. hesternus* displayed a denser and more complex neocortical pattern than *Palaeolama* sp. We observe the first occurrence of a second coronal sulcus branch – the transverse coronal sulcus – just anterior to the original, and a potential third branch between the coronal sulcus and ansate (Fig. 4b), which we cannot confidently identify despite an extensive literature search. At this time, anterior and descending branches of the suprasylvian sulcus converge with the ansate at a single point, more posteriorly than in *Palaeolama* sp. Together with the broader coronal system, this results in a larger, more complex frontal neocortex. Repérant [1971] reported that extant camelids had frontal regions three times larger than they did ~11 Mya. *C. hesternus* appears to have attained a comparable expansion of this area, if not more so (Fig. 5). Further posteriorly, we see a striking difference in the ectolateral sulcus morphology of *C. hesternus* compared to *Palaeolama* sp. The sulcus becomes a system of densely packed short furrows in a mix of horizontal and vertical orientations (accessory ectolaterals), comparable to that in modern camelids and most similar to *Camelus* (Fig. 5c). More peripherally, *C. hesternus* presents the first occurrence of the ascending anterior ectosylvian sulcus, a posterior ectosylvian sulcus located higher on the endocast and separated from the posterior rhinal fissure, and more convoluted oblique sulci 2–3, which together indicate a progressive expansion of the parietal neocortex, specifically of gyrus 2 (Fig. 4e). This region, also known as the sylvian territory, includes areas bounded by the suprasylvian sulcus (dorsally), oblique sulci (posteriorly), and the presylvia sulcus (antero-ventrally) [Barone and Belemlih,

1973]. The accessory sylvian complex is faint on the endocast of *C. hesternus* and we identify it with caution. This would be, potentially, the first appearance of this feature in camelids (Fig. 4e). One feature that apparently remained consistent from the Miocene through the Pleistocene is the general outline of the telencephalon: dorsoventrally deep at its caudal end and progressively shallower towards its anterior (Fig. 3, 4). All three modern genera, however, appear to have a more uniform dorsoventral height throughout the telencephalon. In summary, the frontal and parietal neocortices – regions known for associative functions [Repérant, 1971a] – progressively expand in camelids during the last one million years.

Regarding quantitative aspects, we propose an earlier start to the reported surge in encephalization in the camelid lineage, as measured by EQs [Jerison, 1971; Kruska, 1980]. Jerison [1971] calculated a dramatic rise in camelid encephalization beginning with *C. hesternus* in the late Pleistocene, to modern times. Based on dental proxies, we estimate that *Palaeolama* sp. had a body mass of ~264.5 kg, and *C. hesternus*, ~825.9 kg, yielding similar EQs for both specimens: 0.90 for the former and 0.94 for the latter [Jerison, 1970] (SD1). Given these data, and assuming a generalized rate of brain size change across the camelid lineage, the proposed leap in relative brain size increase began minimally one million years earlier – in the middle Pleistocene – than previously suggested.

Significance of Neocortical Evolution

Among Artiodactyla, Camelidae are recognizable by the peculiar sulcal pattern of the anterior part of their neocortex, cruciate, and intercalaire sulci and by the presence of an arched sulcus and multiple ectolateral sulci [Repérant, 1971a; Orliac et al. 2022]. Prior observations of neocortical evolution in Eocene to Miocene camelids have been described as a systemic evagination of the frontal neocortex out of the sagittal plane, and a simultaneous invagination of dorsal neocortex into the midline [Repérant, 1971a]. Both entolateral and lateral sulci are observable on the dorsal neocortex in Eocene and Oligocene endocasts (Fig. 1a, b). By the Miocene, only the lateral sulcus is visible but it is partially invaginated [Repérant, 1971a]. The new fossils described here indicate that invagination persisted in two different and geographically distinct camelid taxa from two separate points during the Pleistocene. This partial visibility of the lateral sulcus is also clearly evidenced all extant endocasts, supporting Repérant's [1971] theory of medially directed neocortical evolution in this group [Repérant, 1971a]. However, it is worth noting that *C. hesternus* still displays most of the lateral sulcus on the external surface (Fig. 4b). Regarding evagination of the anterior-most part of the neocortex, it is mostly embodied by the dorsal exposure of the intercalaire sulcus. The latter is not visible in *Procamelus* but is present in both *Paleolama* and *Camelops*. These observations in the fossil record provide some support to Reperant's [1971] theory of frontal cortex evagination (extroversion out of the sagittal sinus) occurring in tandem with invagination of the posterior dorsal neocortex [Repérant, 1971a, b].

Ontogenetic developmental work [Repérant, 1971a, p. 7] also provides some support for these evolutionary dynamics considered to be a phenomenon in camelids. Dissections of extant camelid brains show dense fissuration of the neocortex including the entolateral sulcus and other archaic sulci in the sagittal plane at different stages of development [Repérant, 1971a]. Reportedly, the more common pattern is neocortical expansion out of the sagittal plane, ontogenetically and evolutionarily [Repérant, 1971a]. Brain growth encounters physical resistance laterally by the basal ganglia and medially by the corpus collosum [Repérant, 1971a; Striedter and Northcott, 2020]. It plausible that differences in these mechanics were an important factor in the pattern of brain development in camelids, leading to what some consider to be extraordinary neocortical complexity of the camelid brain [Repérant, 1971a]. Further comparison of neocortical gyrification across larger mammalian clades would be needed to support this last statement, and we do not provide those here.

Conclusions

The two Pleistocene camelid endocasts: that of *Palaeolama* sp. from the mid-Pleistocene (~1.2 Mya) of South America and *C. hesternus* from the late Pleistocene (~44 Kya to 11 Kya) of North America, document the first occurrences of neocortical features that are hallmarks of the camelid brain. These are: an external exposure of the intercalaire sulcus, arched sulcus, and complex pattern of multiple ectolateral sulci. These features had been, so far, only observed in modern taxa. The new fossil data provide support for Reperant's [1971a, b] theory of frontal cortex evagination occurring in tandem with invagination of the posterior dorsal neocortex during camelid brain evolution. Regarding quantitative aspects, these two endocasts suggest that a leap in relative brain size increase began minimally one million years earlier – in the middle Pleistocene – than previously suggested [Jerison, 1971]. Our knowledge of camelid brain history during the Pleistocene remains very fragmentary and additional fossil

evidence will allow the drawing of more accurate picture of the recent history that led to the modern camelid brain pattern. Yet, the endocast of *C. hesternus* indicates that by ~ 44 Kya to 11 Kya camelids had reached the "modern stage" of relative brain size and neocortical complexity.

Acknowledgments

We thank Aisling Farrell for providing information and digital data related to *C. hesternus* from the collections at La Brea Tar Pits; Gabriel Aguirre for support and access to collections at the Paleontology Institute and Museum of UZH (PIMUZ); Renaud Lebrun for the access of scanning facilities MRI platform member of the national infrastructure France-BioImaging supported by the French National Research Agency (ANR-10-INBS-04, «Investments for the future»), the LabEx CEMEB (ANR-10-LABX-0004), and NUMEV (ANR-10-LABX-0020); Marcelo Sánchez-Villagra for feedback, edits, and support throughout this project. We thank the editors and anonymous reviewers for their useful comments and improvements to this work. This is ISEM publication number: n° **ISEM 2023-002**

Statement of Ethics

An ethics statement was not required for this study type, no human or animal subjects or materials were used.

Conflict of Interest Statement

We declare we have no competing interests.

Funding Sources

This work was supported by the Swiss National Science Foundation SNF Grant No. 31003A-169395 and the Hubert Curien – Germaine de Staël Grant No. 46776 YE.

Author Contributions

Ana M. Balcarcel: conceptualization, project administration, data collection, methodology, analyses, and writing of original draft; Dylan Bastiaans: segmentation and processing of CT data and review of draft; Maeva J. Orliac: project administration, resources, segmentation and processing of CT data, visualizations, supervision and validation, and writing, review, and editing.

Data Availability Statement

A 3D model of *Palaeolama* sp. is available online at Morphomuseum: https://morphomuseum.com. Electronic supplementary files SD1 and SD2 provide a 3D Adobe Portable Document Format of the *C. hesternus* endocast and all accessory data used in this paper. Further enquiries can be directed to the corresponding author.

References

Barnosky AD, Holmes M, Kirchholtes R, Lindsey E, Maguire KC, Poust AW, et al. Prelude to the anthropocene: two new North American Land mammal ages (NALMAs). Anthropocene Rev. 2014 Dec;1(3):225–42.

Barone R, Belemlih A. Le neopallium du dromadaire (*Camelus dromedarius* L.). Anatom Histol Embryol. 1973;2(4):301–15.

Baskin J, Thomas R. A review of Camelops (mammalia, Artiodactyla, Camelidae), a giant llama from the middle and late Pleistocene (irvingtonian and rancholabrean) of North America. Hist Biol. 2016 Feb 17;28(1–2):120–7.

Buckley M, Lawless C, Rybczynski N. Collagen sequence analysis of fossil camels, Camelops and c.f. Paracamelus, from the Arctic and sub-Arctic of Plio-Pleistocene North America. J Proteomics. 2019 Mar 1;194:218–25.

Cignoni P, Callieri M, Corsini M, Dellepiane M, Ganovelli F, Ranzuglia G. MeshLab: an Open-Source Mesh Processing Tool. Sixth Eurographics Italian Chapter Conference; 2020. p. 12. ed2008.

Damuth JD, MacFadden BJ. Body size in mammalian paleobiology: estimation and biological implications. Cambridge (UK): Cambridge University Press; 1990.

Dechaseaux C. Cervaux d'Animaux Disparu. Paris, FranceEditeurs: Masson et C.; 1962.

Dechaseaux C. Essais de paleoneurologie. Ann de Paleontologie. 1973;59:115–32.

Dechaseaux C. Les debus de l'histoire de la fissration du neopalleum chez les Carnivores et chez les Artiodactyles. Comptes Rendus de l'Academie des Sci. 1968(266):2320–3.

Dechaseaux C. Moulages endocraines d'Artiodactyles primitifs Annales de Paleontologie; 1969. p. 195–248.

Dozo MT. Neuromorfologia de *Utaetus buccatus* (Xenarthra, Dasypodidae): un armadillo del Eoceno temprano de la provincia del Chubut, Argentina. Ameghiniana. 1998;3:285–9.

Edinger T. Brains from 40 million years of camelid history. In: Hassler R, Stephan H, editor. Evolution of the Forebrain. New York: Springer Science and Business Media; 1966. p. 153–61.

Harrison JA. Revision of the Camelinae (Artiodactyla, tylopoda) and description of the new genus alforjas the university of Kansas paleontological contributions. 1979;(95):27.

Hassanin A, Delsuc F, Ropiquet A, Hammer C, Jansen van Vuuren B, Matthee C, et al. Pattern and timing of diversification of Cetartiodactyla (Mammalia, Laurasiatheria), as revealed by a comprehensive analysis of mitochondrial genomes. C R Biol. 2012 Jan;335(1):32–50.

Hay OP. Camels of the fossil genus Camelops. Proc U S Natl Mus. 1913;46(2025):267–77.

Heintzman PD, Zazula GD, Cahill JA, Reyes AV, MacPhee RDE, Shapiro B. Genomic data from extinct North American Camelops revise camel evolutionary history. Mol Biol Evol. 2015 Sep;32(9):2433–40.

Herre W, Thiede U. Studien an gehirnen sudamerikanisther tylopoden. Zoologische Jahrbiicher Abteilung fur Anatomie und Ontogenie Dertiere. 1965;82:155–76.

Honey JG, Harrison JA, Prothero DR, Stevens MS. Camelidae. In: Janis CM, Scott KM, Jacobs LL, editors. Evolution of tertiary mammals of North America Vo 1: Terrestrial Carnivores, Ungulates, and Ungulatelike Mammals. Cambridge: Cambridge University Press; 1998. p. 439–62.

Humpula JF, Ostrom PH, Gandhi H, Strahler JR, Walker AK, Stafford TW, et al. Investigation of the protein osteocalcin of Camelops hesternus: sequence, structure and phylogenetic implications. Geochimica et Cosmochimica Acta. 2007;71(24):5956–67.

Janis CM. Correlation of cranial and dental variables with body size in ungulates and macropodoids. In: Damuth JBJM, editor. Body size in mammalian paleobiology: estimation and biological implications. Cambridge, UK: Cambridge University Press; 1990. p. 255–99.

Jerison HJ. Brain evolution: new light on old principles. Science. 1970;170(3963):1224–5.
Jerison HJ. Quantitative analysis of the evolution of the camelid brain. Am Nat. 1971;105(943):227–39.
Jerison HJ. The theory of encephalization. Annals New York Academy of Sciences. New York: Annals New York Academy of Sciences; 1977. p. 146–60.
Jerison HJ. What fossils tell us about the evolution of the neocortex. In: Kaas JH, editor. Evolution of Nervous systems: Academic Press; 2007. p. 1–12.
Kruska VD. DomestikationsbedingteHirngrößenanderungen bei Säugetieren. J Zoolog Syst Evol Res. 2009;18(3):161–95.
Kruska D. Hirngrößenänderungen bei Tylopoden während der Stammesgeschichte und in der Domestication. (Changes of brain size in Tylopoda during phylogeny and caused by domestication). Verhandlungen der Deutschen Zoologischen Gesellschaft. 1982:173–83.
Lebrun R, Orliac MJ. MorphoMuseuM: an online platform for publication and storage of virtual specimens. The Paleontological Society Paper. 2016 ed. Department of Paleontology of the "Institut des Sciences de l'Évolution" University of Montpellier; 2016. p. 183–95. https://morphomuseum.com/.
Leidy J. Description of a fossil apparently indicating an extinct species of the camel tribe. Proc Acad Nat Sci Phila. 1873;7:172–3.
Lewitus E, Kelava I, Kalinka AT, Tomancak P, Huttner WB. An adaptive threshold in mammalian neocortical evolution. PLoS Biol. 2014 Nov;12(11):e1002000.
Lynch S, Sánchez-Villagra MR, Balcarcel A. Description of a fossil camelid from the Pleistocene of Argentina, and a cladistic analysis of the Camelinae. Swiss J Palaeontol. 2020;139(1):5.
Macrini TE. Description of a digital cranial endocast of Bathygenys reevesi (Merycoidodontidae; Oreodontoidea) and implications for apomorphy-based diagnosis of isolated, natural endocasts. J Vertebr Paleontol. 2009;29(4):1199–211.
Macrini TE, Rowe T, Vandeberg JL. Cranial endocasts from a growth series of Monodelphis domestica (Didelphidae, Marsupialia): a study of individual and ontogenetic variation. J Morphol. 2007 Oct;268(10):844–65.
Orliac MJ, Gilissen E. Virtual endocranial cast of earliest Eocene Diacodexis (Artiodactyla, Mammalia) and morphological diversity of early artiodactyl brains. Proc Biol Sci. 2012 Sep 22;279(1743):3670–7.
Orliac MJ, Maugoust J, Balcarcel AM, Gilissen E. Paleoneurology of Artiodactyla, an Overview of the Evolution of the Artiodactyl Brain. In: Paleoneurology of Amniotes: New Directions in the Study of Fossil Endocasts. Dozo MT., Paulina-Carabajal A., Macrini TE., Walsh S. editors.. Springer International Publishing; 2023. p. 507–555.
Repérant J. Les grandes lignes de l'histoire de la gyrencephalisation chez les camelides; 1971a. p. 658–65.
Repérant J. Morphologie comparee de l'encephale et du moulage endocranien chez les Tylopodes actuels (Mammiferes, Artiodactyles). Bulletin du Muséum national d'histoire naturelle. 1971b;3(4):325.
Repérant J. Les grandes lignes de l'histoire de la gyrencephalisation chez les camélidés. Mammalia. 1971a;35:658–665.
Repérant Jacques. Morphologie comparee de l'encephale et du moulage endocranien chez les Tylopodes actuels (Mammiferes, Artiodactyles). Bulletin du Muséum national d'histoire naturelle. 1971b;3(4):1–325. https://www.biodiversitylibrary.org/ Go to this Web page.
Rook L, Bernor RL, Avilla LS, Cirilli O, Flynn L, Jukar A, et al. Mammal biochronology (Land mammal ages) around the world from late Miocene to middle Pleistocene and major events in horse evolutionary history. Front Ecol Evol. 2019;7.
Roth S. Fossiles de la Pampa, Amerique du Sud; 1889.
Rowe TB, Eiting TP, Macrini TE, Ketcham RA. Organization of the olfactory and respiratory skeleton in the nose of the Gray short-tailed opossum Monodelphis domestica. J Mammal Evol. 2005;12(3–4):303–36.
Rowe TB, Macrini TE, Luo ZX. Fossil evidence on origin of the mammalian brain. Science. 2011 May 20;332(6032):955–7.
Scherer CS. The Camelidae (mammalia, Artiodactyla) from the quaternary of South America: cladistic and biogeographic hypotheses. J Mammal Evol. 2012;20(1):45–56.
Schulthess B. Beiträge zur Kenntnis der Xenarthra auf Grund der Santiago Roth'schen Sammlung des Zoologischen Museums der Universität Zürich. Imprimerie Albert Kundig; 1920. p. 58–9.
Scott WB, Jepsen GL. The mammalian fauna of the white river Oligocene: Part IV. Artiodactyla. Trans Am Philosophical Soc. 1940;28(4):363–746.
Striedter GF, Northcott RG. Brains through time: a natural history of vertebrates. New York, USA: Oxford University Press; 2020.
Verzi DH, Deschamps CM, Tonni EP. Biostratigraphic and palaeoclimatic meaning of the middle Pleistocene South American rodent Ctenomys kraglievichi (caviomorpha, octodontidae). Palaeogeogr Palaeoclimatol Palaeoecol. 2004;212(3–4):315–29.
Webb DS. The osteology of Camelops. Bull Los Angeles County Mus. 1965;1:50.
Wortman MD. The extinct Camelidae of North America and some associated forms. Bull Am Mus Nat Hist. 1898;X:93–143.
Zazula GD, Turner DG, Ward BC, Bond J. Last interglacial western camel (Camelops hesternus) from eastern Beringia. Quat Sci Rev. 2011 Sep;30(19–20):2355–60.